ACS Catalysis

Letter

pubs.acs.org/acscatalysis

Photoinduced Hydrogen Evolution Catalyzed by a Synthetic Diiron Dithiolate Complex Embedded within a Protein Matrix

Akira Onoda,* Yoshihiko Kihara, Kazuki Fukumoto, Yohei Sano, and Takashi Hayashi*

Department of Applied Chemistry, Graduate School of Engineering, Osaka University, Suita, Osaka 565-0871, Japan

Supporting Information

ABSTRACT: The hydrogen-evolving diiron complex, $(\mu\text{-S})_2Fe_2(CO)_6$ with a tethered maleimide moiety was synthesized and covalently embedded within the cavity of a rigid β-barrel protein matrix by coupling a maleimide moiety to a cysteine residue within the β-barrel. The $(\mu\text{-S})_2Fe_2(CO)_6$ core within the cavity was characterized by UV−vis absorption and a characteristic CO vibration determined by IR measurements. The diiron complex embedded within the cavity retains the necessary catalytic activity (TON up to 130 for 6 h) to evolve H_2 via a photocatalytic cycle with a Ru photosensitizer in a solution of 100 mM ascorbate and 50 mM Tris/HCl at pH 4.0 and 25 °C.

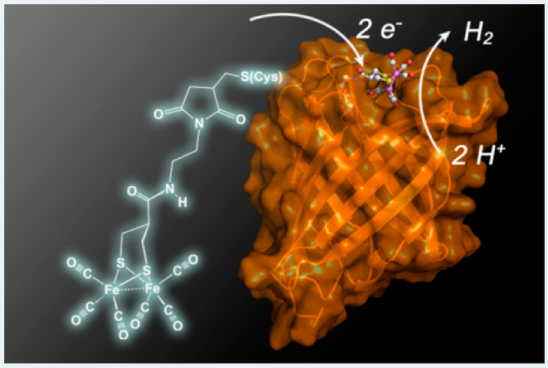

KEYWORDS: *hydrogenase, hybrid catalysts, artificial metalloenyzme, photoinduced hydrogen evolution, diiron dithiolato complex, nitrobindin, β-barrel protein*

Hydrogenase catalyzes the reduction of protons and the capture of electrons from H_2 under mild conditions.[1] The active site of [FeFe]-H_2ase, which is known as an H-cluster, is formed by an unusual bridging dithiolate ligand and diatomic ligands, such as carbonyls and cyanates. This arrangement contributes to the structural stability and the reactivity of the H-cluster.[2] To understand the structural and functional basis of the diiron active site, a variety of sophisticated H-cluster model complexes containing a diiron carbonyl cluster ($(\mu\text{-S})_2Fe_2(CO)_n$) have been studied.[3] Furthermore, since the model complex of the H-cluster requires electrons to produce H_2 from protons, a single- or multicomponent photochemical system in which electrons are cascaded to the diiron cluster has been constructed using a visible light-driven photosensitizer.[4]

Combining the $(\mu\text{-S})_2Fe_2(CO)_n$ model with biological scaffolds such as peptides and proteins to further optimize the surrounding environment of the diiron core is another strategy that has attracted much attention.[5] These scaffolds are also advantageous in the effort to solubilize the catalysts.[3c,d,6] Jones et al. have reported a structural hydrogenase model with a $(\mu\text{-S})_2Fe_2(CO)_6$ core that includes two cysteine thiolate ligands in a C*X*X*C* motif of a synthetic peptide. We previously reported that a $(\mu\text{-}S\text{-Cys})_2Fe_2(CO)_6$ core in the artificial C*X*X*C* motif engineered in cytochrome *c* protein produces H_2 photocatalytically.[7] Ghirlanda et al. developed a bioinspired peptide-based catalyst containing a diiron cluster supported by artificial dithiol amino acid ligands.[8] Herein, we report the preparation and characterization of an iron−carbonyl complex, $(\mu\text{-S})_2Fe_2(CO)_6$, covalently attached to the cavity of a β-barrel protein as an artificial hydrogenase (Figure 1). Furthermore, we demonstrate photocatalytic H_2 production using this artificial hydrogenase supported by $[Ru(bpy)_3]^{2+}$ as a photosensitizer in the presence of ascorbate, a sacrificial reagent.

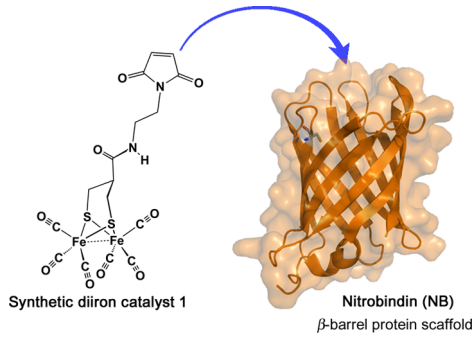

Figure 1. Preparation of a diiron complex-linked nitrobindin catalyst.

We designed a diiron complex with a dithiolate ligand as a functional active site model of a hybrid H_2-evolving catalyst. To anchor the diiron complex onto the specific site of the protein, we used a dithiolate with a maleimide group that forms a covalent linkage to a Cys residue, as shown in Figure 1. The diiron catalyst **1** with the maleimide group was synthesized from a diiron hexacarbonyl complex (which includes a 2-carboxy-1,3-propanedithiol ligand)[9] by coupling it to an amino group of a maleimide precursor compound (Supporting

Received: March 25, 2014
Revised: June 11, 2014
Published: July 9, 2014

   dx.doi.org/10.1021/cs500392e | ACS Catal. 2014, 4, 2645−2648

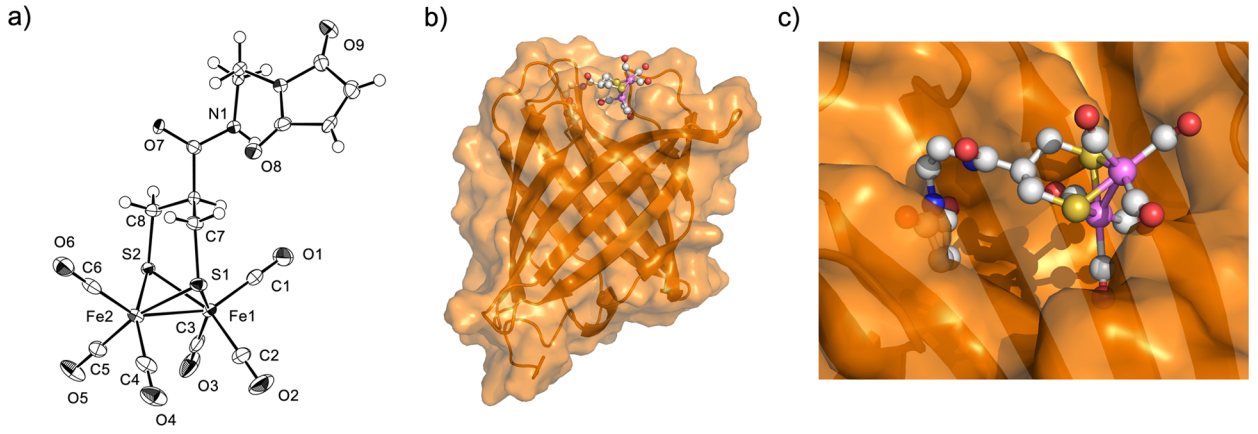

Figure 2. (a) Crystal structure of **1** (50% probability ellipsoids). Selected bond lengths (Å) and angles (°): Fe1−Fe2, 2.5183(3); Fe1−S1, 2.2657(4); Fe1−S2, 2.2470(4); Fe2−S1, 2.2580(4); Fe2−S2, 2.2391(3); S1−C7, 1.8333(16); S2−C8, 1.8236(16); Fe1−C1, 1.8092(18); Fe1−C2, 1.802(2); Fe1−C3, 1.75(2); Fe2−C4, 1.8139(19); Fe2−C5, 1.7980(18); Fe2−C6, 1.8054(17); C1−O1, 1.129(2); C2−O2, 1.136(2); O3−O3, 1.144(2); C4−O4, 1.139(2); C5−O5, 1.138(2); C6−O6, 1.131(2); Fe1−S1−Fe2, 67.655(12); Fe1−S2−Fe2, 68.299(13). (b) Side view and (c) zoomed view of the structure of NB-**1** calculated by YASARA.[10] Iron in violet, sulfur in yellow, carbon in white, oxygen in red, and nitrogen in blue.

Information (SI) Scheme S1). Catalyst **1** was characterized by ESI-TOF-MS and ^{1}H NMR spectroscopy (SI Figure S1). The crystal structure analysis reveals that the dithiolate ligand binds to two iron atoms in the typical coordination mode commonly found in the analogous $(\mu\text{-S})_2Fe_2(CO)_6$ complexes (Figure 2a).

Next, to incorporate the diiron complex **1**, a rigid protein scaffold containing a suitably sized cavity is used as a host. Here, a β-barrel structure is expected to provide an appropriate structural motif in various protein scaffolds. We thus selected nitrobindin (NB), which contains a heme moiety within the cavity surrounded by eight β-strands. Such a β-barrel structure provides a remarkably rigid platform to construct an artificial active site because proteins of the NB family retain their inherent barrel folding even in an apo form obtained by removal of the heme cofactor.[11] Our previous study identified Gln96 as a possible single anchoring site.[12] This residue, which is located on the entrance of the cavity in NB, was mutated to a Cys residue for covalently binding the diiron complex **1** through the maleimide moiety. According to the X-ray crystal structure of **1**, the molecular size of **1** appears suitable for anchoring within the cavity (Figure 2b,c).

The Q96C-NB protein expressed in *Escherichia coli* was obtained as the apo form and purified using a His tag affinity column. The tag was cleaved by Factor Xa, and the protein was purified using a His tag affinity column and a benzamidine-linked Sepharose 6B column. The purified Q96C-NB protein was characterized by SDS−PAGE and ESI-TOF-MS (SI Figure S2 and S3). The protein solution was then supplemented with DTT to reduce the thiol group of Cys96. The reduced NB protein was concentrated and purified using a HiTrap desalting column equilibrated with 50 mM Tris/HCl (pH 8.0). The collected NB protein solution was slowly supplemented with **1** in acetonitrile, and the mixed solution was incubated at room temperature for 1 h. The solution was concentrated and passed through a desalting column to remove the unreacted complex, yielding the NB-**1** hybrid catalyst. The conjugation efficiency was confirmed to be 78% on the basis of the protein and Fe concentrations determined by Bradford assay and ICP-OES, respectively. The reaction between the Cys96 and the maleimide moiety in **1** proceeds smoothly, although the Cys residue could be involved in coordination to the iron atoms.

The conjugation between **1** and NB was confirmed by UV−vis spectra, as shown in Figure 3. The UV−vis absorption

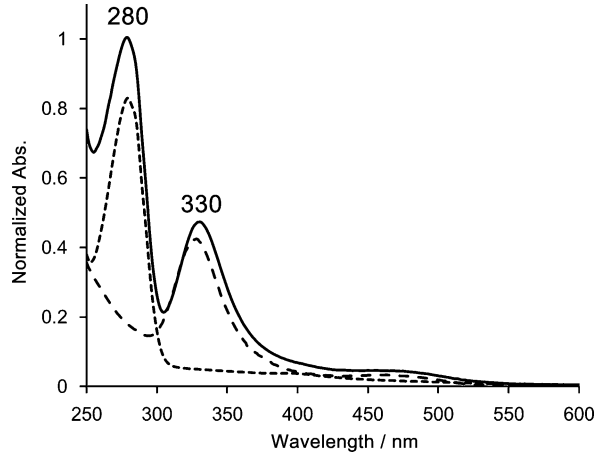

Figure 3. UV−vis absorption spectra of NB−**1** in 50 mM Tris/HCl buffer at pH 8 (solid line), the apo form of NB (dotted line), and **1** in acetonitrile (broken line).

spectrum of NB-**1** indicates that the diiron complex **1** is incorporated into the protein matrix. The MALDI-TOF-MS spectrum of NB-**1** showed the desired molecular weight of the corresponding protein with the covalently linked diiron moiety (calcd 18797.99, found 18798.88), although the CO ligands dissociate under the ionization conditions of MALDI-TOF-MS (SI Figure S4). Moreover, it is known that the CO ligands of hydrogenase models of the H-cluster provide characteristic absorptions in the IR region at 1800−2200 cm^{-1}. Figure 4a shows the FT-IR spectrum of the diiron complex NB-**1** with three characteristic bands assignable to the CO ligands at 2077, 2037, and 2005 cm^{-1}. The positions and the shapes of these bands are similar to those observed for **1** (Figure 4b). This confirms that the six CO ligands coordinate to the $(\mu\text{-S-Cys})_2Fe_2$ core, which is covalently linked to the protein cavity.[3b,c] The subtle spectral changes in the vicinity of 2000 cm^{-1} suggest that the CO ligands interact with the neighboring amino acid residues.

dx.doi.org/10.1021/cs500392e | *ACS Catal.* 2014, 4, 2645−2648

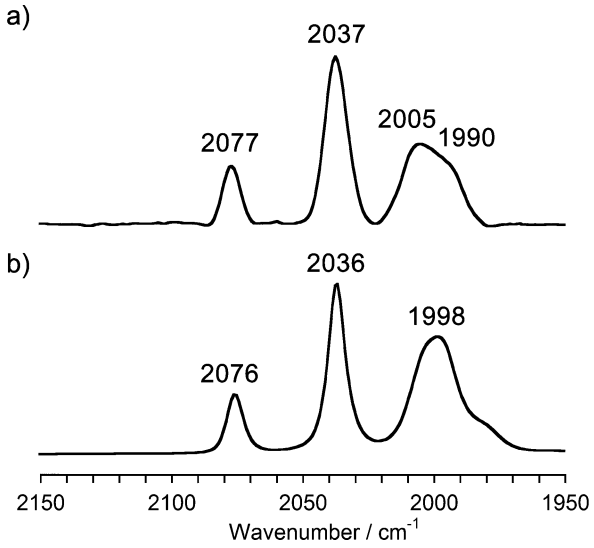

Figure 4. FT-IR spectra of (a) NB-**1** (300 μM NB-**1** in 50 mM Tris/HCl buffer at pH 8) and (b) **1** in methanol.

Next, photochemical H_2 evolution experiments were performed with NB-**1** in the presence of excess ascorbate as a sacrificial donor and photosensitizer (Figure 5). The photo-

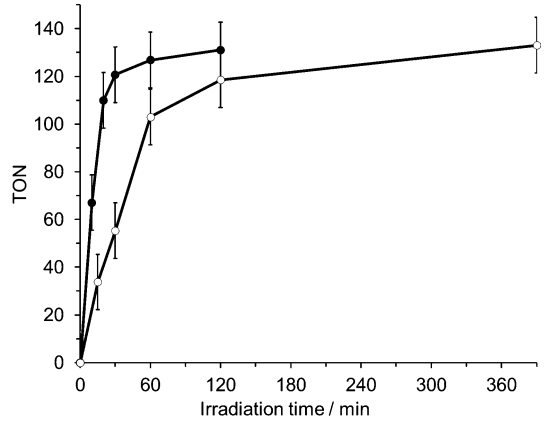

Figure 5. Visible light-driven H_2 generation by NB-**1** in 50 mM Tris/HCl (pH 4.0) (open circles) and **1** in 50 mM Tris/HCl (pH 4.0) containing 4% (v/v) THF (solid circles) at 25 °C.[13]

catalytic production of H_2 reached a plateau after 6 h, yielding a turnover number of ~130 per the hybrid catalyst with a maximum turnover frequency of ~2.3/min calculated from the initial rate of the H_2 evolution.[13] The reaction by the complex **1** without the protein matrix was performed under similar conditions, including 4% (v/v) THF. The result clearly indicates that the $(\mu$-*S*-Cys$)_2Fe_2(CO)_6$ core within the protein environment retains catalytic activity of the photocatalytic H_2 evolution, although the reaction within the protein would be decelerated owing to decreased accessibility of the ruthenium photosensitizer to the diiron active site. In fact, H_2 evolution was not observed in the absence of $[Ru(bpy)_3]^{2+}$, indicating that the ruthenium complex plays a role as a photosensitizer.

The effect of pH on H_2 evolution was also investigated. Increasing the pH value to 7.8 led to degradation of the activity to 28% of maximal H_2 evolution due to a decrease in the proton concentration. Lowering the pH value to 3.2 resulted in loss of the activity to 18% as a result of inactivation of ascorbate (pK_a = 4.0) as the sacrificial reagent for $[Ru(bpy)_3]^{2+}$. NB-**1** optimally functions as a catalyst for H_2 evolution near pH 4.7, at which the proton and ascorbate concentrations are both optimal for the reaction.[7]

In conclusion, we describe a new $(\mu$-S$)_2Fe_2(CO)_6$ complex, which can be covalently embedded within the cavity of a protein matrix. Interestingly, the diiron complex embedded at the side of the cavity of NB evolves H_2 via the photocatalytic cycle with Ru photosensitizer under mild conditions in aqueous media. We are now engaged in improving the activity of photocatalytic H_2 evolution by engineering of the amino acid residues within the cavity of the protein.

■ ASSOCIATED CONTENT

Supporting Information

Experimental section, crystallographic data, ^{1}H NMR and ^{13}C NMR spectra of the diiron complex **1**, SDS-PAGE and ESI-TOF-MS analyses of the NB protein, MALDI-TOF-MS spectrum of NB-**1**. CCDC 991641 (**1**). This material is available free of charge via the Internet at http://pubs.acs.org.

■ AUTHOR INFORMATION

Corresponding Authors

*E-mail: onoda@chem.eng.osaka-u.ac.jp.
*E-mail: thayashi@chem.eng.osaka-u.ac.jp.

Notes

The authors declare no competing financial interest.

■ ACKNOWLEDGMENTS

This work was financially supported by the JSPS Japan-German Graduate Externship Program, DFG through the International Reserch Training Group "Selectivity in Chemo-and Biocatalysts (Seleca)", and Grants-in-Aid for Scientific Research (Innovative Areas "Molecular Activation", area 2204) from MEXT. K.F. expresses his special thanks to the JSPS Japanese-German Graduate Externship Program on "Environmentally Benign Bio- and Chemical Processes" for financial support of his stay in RWTH Aachen. We acknowledge Dr. H. Sugimoto and Prof. S. Itoh at the Department of Materials and Life Science, Graduate School of Engineering, Osaka University for crystallographic structural analysis.

■ REFERENCES

(1) (a) *Hydrogen As a Fuel: Learning from Nature*; Cammack, R.; Frey, M.; Robson, R., Eds.; CRC Press: Boca Raton, FL, 2002. (b) *Energy··· beyond Oil*; Armstrong, F., Blundell, K., Eds.; Oxford University Press: Oxford, 2007.

(2) (a) Peters, J. W. *Science* **1998**, *282*, 1853−1858. (b) Nicolet, Y.; Piras, C.; Legrand, P.; Hatchikian, C. E.; Fontecilla-Camps, J. C. *Structure* **1999**, *7*, 13−23. (c) Pandey, A. S.; Harris, T. V.; Giles, L. J.; Peters, J. W.; Szilagyi, R. K. *J. Am. Chem. Soc.* **2008**, *130*, 4533−4540.

(3) (a) Tard, C.; Liu, X.; Ibrahim, S. K.; Bruschi, M.; De Giola, L.; Davies, S. C.; Yang, X.; Wang, L. S.; Sawers, G.; Pickett, C. J. *Nature* **2005**, *433*, 610−613. (b) Jones, A. K.; Lichtenstein, B. R.; Dutta, A.; Gordon, G.; Dutton, P. L. *J. Am. Chem. Soc.* **2007**, *129*, 14844−14845. (c) Singleton, M. L.; Reibenspies, J. H.; Darensbourg, M. Y. *J. Am. Chem. Soc.* **2010**, *132*, 8870−8871. (d) Singleton, M. L.; Crouthers, D. J.; Duttweiler, R. P.; Reibenspies, J. H.; Darensbourg, M. Y. *Inorg. Chem.* **2011**, *50*, 5015−5026. (e) Wang, N.; Wang, M.; Wang, Y.; Zheng, D.; Han, H.; Ahlquist, M. S. G.; Sun, L. *J. Am. Chem. Soc.* **2013**, *135*, 13688−13691. (f) Hsieh, C.-H.; Erdem, Ö. F.; Harman, S. D.; Singleton, M. L.; Reijerse, E.; Lubitz, W.; Popescu, C. V.; Reibenspies, J. H.; Brothers, S. M.; Hall, M. B.; Darensbourg, M. Y. *J. Am. Chem. Soc.* **2012**, *134*, 13089−13102. (g) Camara, J. M.; Rauchfuss, T. B. *Nat.*

Chem. **2012**, *4*, 26−30. (h) Berggren, G.; Adamska, A.; Lambertz, C.; Simmons, T. R.; Esselborn, J.; Atta, M.; Gambarelli, S.; Mouesca, J. M.; Reijerse, E.; Lubitz, W.; Happe, T.; Artero, V.; Fontecave, M. *Nature* **2013**, *499*, 66−69. (i) Esselborn, J.; Lambertz, C.; Adamska-Venkatesh, A.; Simmons, T.; Berggren, G.; Noth, J.; Siebel, J.; Hemschemeier, A.; Artero, V.; Reijerse, E.; Fontecave, M.; Lubitz, W.; Happe, T. *Nat. Chem. Biol.* **2013**, *9*, 607−609. (j) Happe, T.; Hemschemeier, A. *Trends Biotech.* **2014**, *32*, 170−176.

(4) (a) Tard, C.; Pickett, C. J. *Chem. Rev.* **2009**, *109*, 2245−2274. (b) Sun, L.; Åkermark, B.; Ott, S. *Coord. Chem. Rev.* **2005**, *249*, 1653−1663. (c) Ott, S.; Kritikos, M.; Åkermark, B.; Sun, L. *Angew. Chem., Int. Ed.* **2003**, *42*, 3285−3288. (d) Ekström, J.; Abrahamsson, M.; Olson, C.; Bergquist, J.; Kaynak, F. B.; Eriksson, L.; Sun, L.; Becker, H. C.; Åkermark, B.; Hammarström, L.; Ott, S. *Dalton Trans.* **2006**, 4599−4606. (e) Song, L. C.; Tang, M. Y.; Mei, S. Z.; Huang, J. H.; Hu, Q. M. *Organometallics* **2007**, *26*, 1575−1577. (f) Li, X.; Wang, M.; Zhang, S.; Pan, J.; Na, Y.; Liu, J.; Åkermark, B.; Sun, L. *J. Phys. Chem. B* **2008**, *112*, 8198−8202. (g) Na, Y.; Pan, J.; Wang, M.; Sun, L. *Inorg. Chem.* **2007**, *46*, 3813−3815. (h) Na, Y.; Wang, M.; Pan, J.; Zhang, P.; Åkermark, B.; Sun, L. *Inorg. Chem.* **2008**, *47*, 2805−2810. (i) Streich, D.; Astuti, Y.; Orlandi, M.; Schwartz, L.; Lomoth, R.; Hammarström, L.; Ott, S. *Chem.—Asian J.* **2010**, *16*, 60−63. (j) Zhang, P.; Wang, M.; Na, Y.; Li, X.; Jiang, Y.; Sun, L. *Dalton Trans.* **2010**, *39*, 1204−1206. (k) Nann, T.; Ibrahim, S. K.; Woi, P. M.; Xu, S.; Ziegler, J.; Pickett, C. J. *Angew. Chem., Int. Ed.* **2010**, *49*, 1574−1577. (l) Eckenhoff, W. T.; Eisenberg, R. *Dalton Trans.* **2012**, *41*, 13004−13021.

(5) Faiella, M.; Roy, A.; Sommer, D.; Ghirlanda, G. *Pept. Sci.* **2013**, *100*, 558−571.

(6) (a) Wang, F.; Wang, W. G.; Wang, X. J.; Wang, H. Y.; Tung, C. H.; Wu, L. Z. *Angew. Chem., Int. Ed.* **2011**, *50*, 3193−3197. (b) Cao, W. N.; Wang, F.; Wang, H. Y.; Chen, B.; Feng, K.; Tung, C. H.; Wu, L. Z. *Chem. Commun.* **2012**, *48*, 8081−8083.

(7) (a) Sano, Y.; Onoda, A.; Hayashi, A. *J. Inorg. Biochem.* **2012**, *108*, 159−162. (b) Sano, Y.; Onoda, A.; Hayashi, T. *Chem. Commun.* **2011**, *47*, 8229−8231.

(8) Roy, A.; Madden, C.; Ghirlanda, G. *Chem. Commun.* **2012**, *48*, 9816−9818.

(9) (a) Thomas, C. M.; Rüdiger, O.; Liu, T.; Carson, C. E.; Hall, M. B.; Darensbourg, M. Y. *Organometallics* **2007**, *26*, 3976−3984. (b) Volkers, P. I.; Rauchfuss, T. B.; Wilson, S. R. *Eur. J. Inorg. Chem.* **2006**, *2006*, 4793−4799.

(10) Krieger, E.; Darden, T.; Nabuurs, S.; Finkelstein, A.; Vriend, G. *Proteins: Struct. Funct. Bioinf.* **2004**, *57*, 678−683.

(11) (a) Amoia, A. M.; Montfort, W. R. *Protein Sci.* **2007**, *16*, 2076−2081. (b) Phillips, G. N.; Bianchetti, C. M.; Blouin, G. C.; Bitto, E.; Olson, J. S. *Proteins: Struct. Funct. Bioinf.* **2010**, *78*, 917−931.

(12) (a) Onoda, A.; Fukumoto, K.; Arlt, M.; Bocola, M.; Schwaneberg, U.; Hayashi, T. *Chem. Commun.* **2012**, *48*, 9756−9758. (b) Fukumoto, K.; Onoda, A.; Mizohata, E.; Bocola, M.; Inoue, T.; Schwaneberg, U.; Hayashi, T. *ChemCatChem* **2014**, *6*, 1229−1235.

(13) The H_2 evolved was identified and quantified by gas chromatography. A standard reaction was carried out by mixing NB-**1** (7.8 μM) containing $[Ru(bpy)_3]^{2+}$ (140 μM) as a photosensitizer in a solution of 100 mM ascorbate and 50 mM Tris/HCl at pH 4.0. In a quartz cell equipped with a Teflon septum screw cap, an anaerobic reaction solution was irradiated with a Xe lamp equipped with UV- (<410 nm) and IR- (>770 nm) cutoff filters at 25 °C, and the headspace gas was analyzed for H_2 evolution.